Photoluminescence from an individual single-walled carbon nanotube

J. Lefebvre,[1,*] J. M. Fraser,[1] P. Finnie,[1] and Y. Homma[2]
[1]*Institute for Microstructural Sciences, National Research Council, Montreal Road, Ottawa, Ontario, K1A OR6, Canada*
[2]*NTT Basic Research Laboratories, Nippon Telegraph and Telephone Corporation, 3-1 Morinosato-Wakamiya, Atsugi, Kanagawa 243-0198, Japan*
(Received 15 July 2003; published 10 February 2004)

Photoluminescence (PL) and photoluminescence excitation (PLE) spectra are obtained from individual single-walled carbon nanotubes (SWNTs). Individual SWNT spectra are compared with spectra from ensembles. The PL spectrum of an individual SWNT in air at room temperature has a single asymmetric peak of width typically 10 to 15 meV, with no detected background. Both absorption and emission are strongly polarized along the tube axis. Photoluminescence excitation spectroscopy on single SWNTs clearly confirms the unique, one-to-one association of optical absorption resonances with individual emission peaks. Resonances in the PLE spectra are typically ≈ 30 meV wide, with the PL intensity enhanced tenfold over nonresonant excitation. Whether for emission or absorption, the peak shape and peak width are almost the same for a single nanotube as they are for the corresponding species in a large ensemble. That is, there is no significant inhomogeneous broadening. While ensemble measurements are complicated by the superposition of many PL peaks from many different species, single nanotube spectra clearly isolate a single peak and are thus simpler to interpret.

DOI: 10.1103/PhysRevB.69.075403 PACS number(s): 78.67.Ch, 78.55.−m, 78.66.Tr

The past decade of research on single-walled carbon nanotubes (SWNTs) has resulted in many outstanding scientific findings, some with anticipated impact in tomorrow's technology.[1] The intriguing properties of the SWNT stem from its simple, rigid, nanometer-scale structure, a single layer of carbon atoms rolled up into a seamless cylinder. The various configurations of carbon atoms on the surface of a cylinder are uniquely classified using roll-up vector indices, or alternatively by a specific diameter and chiral angle. To first order, theory predicts that two-thirds of SWNTs are semiconductors. Semiconducting nanotubes have a direct band gap in momentum space with a diameter/chirality dependent energy. In a direct band gap semiconductor, where no momentum transfer is necessary for an interband transition, the likelihood of light emission from electron-hole recombination is high.

Despite the theoretical promise, it was only recently that SWNTs were found to emit light from interband recombination of electron-hole pairs. Last year, a group at Rice University prepared a solution in which SWNTs were individually isolated in micelles. Upon illumination, infrared photoluminescence (PL) was detected from the ensemble of isolated nanotubes in solution, and it was clearly demonstrated that the light was from electron-hole recombination at the band edge.[2,3] Shortly after, we found that ensembles of bare SWNTs suspended in air also emit band gap PL.[4] In both cases the key is to isolate the nanotubes, minimizing interaction with their environment. Moving beyond ensemble measurements, we report the PL spectroscopy made on a single, isolated SWNT. At the single nanotube level, the spectra are simpler and free from ambiguities inherent in ensemble measurements. The one-dimensional character of SWNTs should have a dramatic influence on their optical properties,[5–7] and this character is readily apparent in single SWNT PL spectroscopy.

Here, chemical vapor deposition with a pure methane precursor is used to synthesize the SWNTs.[8] Growth temperatures range from 800 °C to 900 °C. To suspend nanotubes, pillar patterns on the substrate are used. A thermal SiO_2 coating on Si substrates is patterned into SiO_2 pillars using electron beam lithography and reactive ion etching. The pillars and the surrounding substrate surface below are coated with ~ 1 nm of evaporated iron or cobalt. Such films are good catalysts for SWNT growth,[8] and PL measurements on individual nanotubes grown with either catalyst gives the same result. After growth, scanning electron microscope (SEM) observations reveal SWNTs from all metal-coated surfaces, and of interest here, SWNTs suspended between neighboring pillars.[9] Since isolation is key to SWNT luminescence, only suspended SWNTs are observed to emit PL.[4]

Figure 1 shows SEM images of isolated pillar pairs and suspended SWNTs. Figure 1(a) shows a pillar pair at an angle of $\sim 35°$, while Fig. 1(b) shows another pair in plan view. In both images, many SWNTs are visible, but a single, long tube bridges the pillars. Figure 1(a) shows a long SWNT that bridges to another, shorter SWNT rather than bridging pillar to pillar, strictly speaking. The long SWNT in Fig. 1(b) does completely bridge the pillars. It is important to note that both nanotubes are at least somewhat curved. Curvature may have some influence on the details of the PL, as will be discussed below.

Photoluminescence from individual SWNTs is obtained with a micro-PL apparatus in which both the exciting laser beam and collected light pass through the same microscope objective. Pillar pairs spaced by ~ 1 μm and well separated from other pillar pairs by about 30 μm are used for single nanotube spectroscopy. With a laser beam tightly focused to a ~ 2 μm in diameter spot size, it is straightforward to address a single pillar pair. For the purpose of comparison with nanotube ensembles, measurements from uniform arrays of closely spaced pillars are also presented. In the same

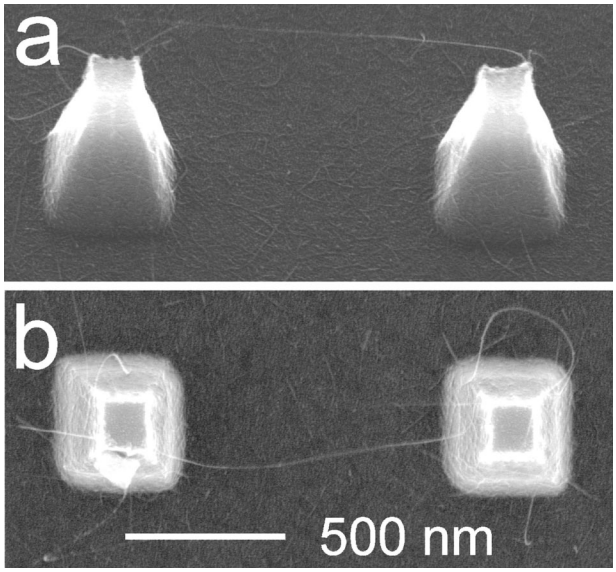

FIG. 1. Scanning electron micrograph of SWNTs suspended between SiO_2 pillars. (a) View from a $\sim 35°$ angle. (b) Plan view. Individual SWNTs that bridge pillar pairs can be slightly bowed.

micro-PL configuration, an aspheric lens replaces the microscope objective, producing a larger $\sim 100\ \mu$m diameter spot size. PL was excited with different lasers in continuous wave mode, including a tunable Ti:sapphire laser (725 to 837 nm, 2 W maximum output power). All spectra presented here are taken in a low power density (< 0.1 MW/cm^2) regime, for which the PL intensity grows linearly with excitation power density, with no change in peak shape. The luminescence is dispersed by a single grating spectrometer (149 grooves/mm, 1250 nm blaze) onto a liquid nitrogen cooled InGaAs 512 photodiode array with sensitivity from visible to 1650 nm (0.75 eV). With the spectrometer at 1240 nm (1 eV), a spectrum covers the 900–1555 nm wavelength range (0.80–1.38 eV) with a resolution of about 1 nm (~ 1 meV). Spectra are typically integrated over a 30 s accumulation time.

The PL from several different individual SWNTs is presented in Fig. 2. Each is suspended between pillars in air at room temperature. The peak height is normalized to unity. In all cases, the PL spectrum from an individual SWNT is dominated by one narrow peak. The emission energy spans the 0.75 to 1.1 eV range, limited at low energy by the detector sensitivity and at high energy by the SWNT species that are present and luminescent. It is worth noting that scanning over many pillar pairs, many of the same PL peaks are seen again and again, suggesting that the same nanotube species is present in many spatially separated sites. This also suggests that the emission energy is a robust property of each nanotube species.

The full width at half maximum (FWHM) of the PL peak is typically 10–15 meV, substantially smaller than the thermal energy (k_BT) at room temperature of 25 meV. The lineshape is found to be asymmetric. Of hundreds of peaks surveyed, in almost every case the peak had a sharp rise on the low-energy side, and a more gradual fall off to zero at high energies. Figure 1(b) shows that a Lorentzian function provides an excellent fit for the high-energy side of the peak,

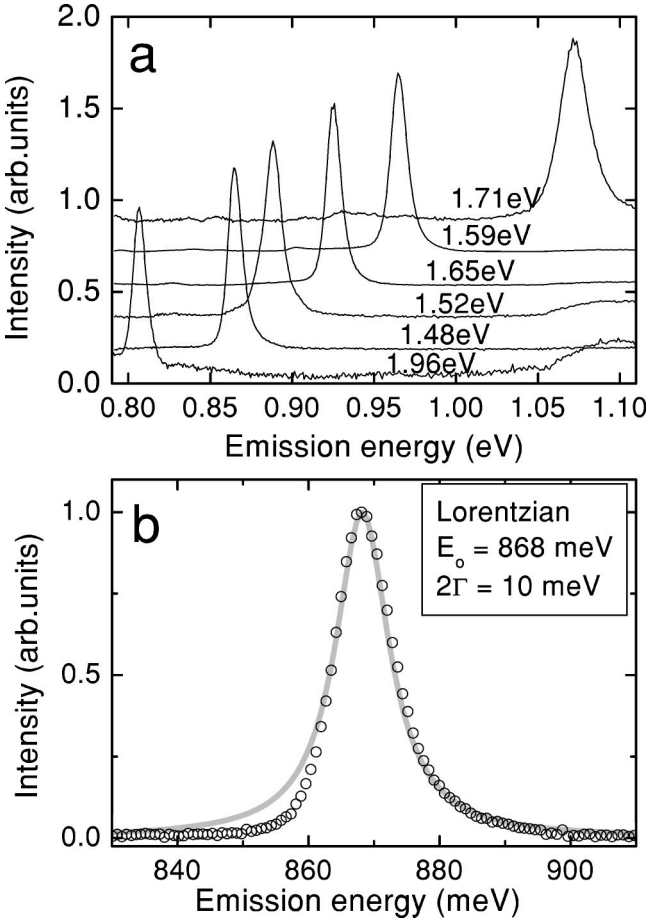

FIG. 2. Photoluminescence (PL) spectra from individual SWNTs. (a) PL spectra from several different nanotubes in air at 300 K. SWNTs have emission energy between 0.75 and 1.1 eV with typically 10–15 meV linewidth. Spectra are normalized to unity and offset for clarity. The laser excitation energy for each curve is indicated. Spectra are taken with ~ 1 mW excitation power, with a $\sim 2\ \mu$m spot diameter. The broad feature above 1.06 eV, especially prominent in the red and green curves, arises from the Si substrate. The relative strength of the SWNT PL intensity makes it invisible on the other curves. (b) The second curve from the bottom plotted on an enlarge scale together with a Lorentzian functional form.

and accentuates the steeper drop to lower energies. The particular peak shown here is typical, having 55% of its spectral weight above the peak maximum. The sharp asymmetric lineshape is consistent with the shape of van Hove singularities in the joint density of states.

While this work was under review, PL was reported from single SWNTs suspended in soap micelles and spun on to a substrate.[10] There are striking differences between PL data presented here and that study. The linewidths are two to three times broader in that work, and the lineshape was symmetric and Lorentzian. Very occasionally we found peaks of widths approaching those of Ref. 10, but such broad peaks are exceptional, and none were completely symmetric. The nanotubes in Ref. 10 were shorter and narrower than the ones studied here, and these are possible causes of the broadening. Some evidence for this is that the small diameter nanotube in Fig. 2 with emission at 1.073 eV is broader than the other

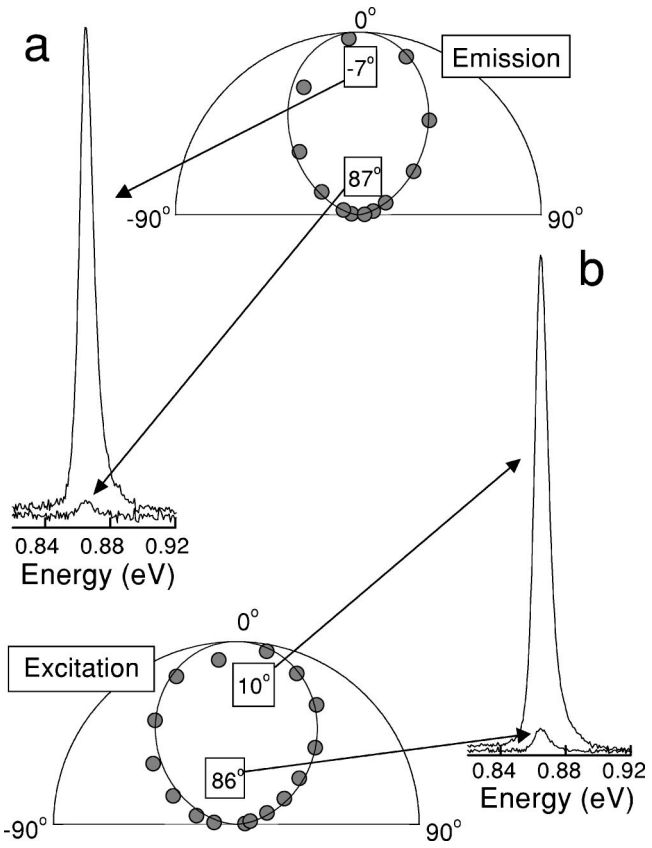

FIG. 3. Polarization dependence of the photoluminescence (PL) intensity. (a) Polarization resolved emission. At the left, examples of spectra are shown for two different polarization angles. On the polar plot, the PL integrated intensity is shown as a function of the angle between the nanotube axis and a linear polarizer. The solid line represents a $\cos^2\theta$ function. (b) Polarization resolved excitation. At the right, examples of spectra are shown for two different angles of the laser polarization angle. The angle of the linearly polarized laser excitation (600:1 extinction ratio) is rotated using a half-wave plate. On the polar plot, the PL integrated intensity is shown as a function of the angle between the nanotube axis and the laser polarization angle. The solid line represents a $[\cos^2\theta]^{0.7}$ function. For both (a) and (b), a 0.5 mW excitation at 1.481 eV was focussed to a $\sim 2\ \mu$m diameter spot.

peaks. However, such small diameter nanotubes were rare in our case, so the evidence is inconclusive. Another cause for the broadening in Ref. 10 may be environmental effects. This seems quite likely because for the micelle encapsulated nanotubes, the peak widths for single nanotubes and ensembles were comparable. We will show below that the same is true for nanotubes suspended in air.

For a single straight nanotube, emission and absorption of light should be preferentially polarized along the nanotube axis. Polarized emission of light from individual nanotubes has been reported very recently,[10,11] and effects of polarized absorption have been shown in Raman studies of individual nanotubes.[12] Here, the nanotubes have $\sim 1000{:}1$ aspect ratios, and optical transitions should be sensitive probes of this large anisotropy. In this work, polarized absorption and polarized emission are each separately demonstrated for the same SWNT.

Polarization resolved PL measurements on an individual SWNT are shown in Fig. 3. In Fig. 3(a), for emission the PL intensity is recorded as a function of the angle between the nanotube axis and a linear polarizer. Emission reaches a maximum around 0°, which corresponds to the electric component of the light field along the tube axis. A simple $\cos^2\theta$, shown as a solid line in the angular plot, is a good fit to the data. However, the intensity never falls exactly to zero, and the extinction ratio (maximum to minimum intensity) falls within a range between 10 and 20. Since SWNTs are found to be slightly bowed between pillars (see Fig. 1), it seems plausible that a perfectly straight SWNT might have a higher extinction ratio than that measured here.

The excitation polarization dependence of the PL intensity is shown in Fig. 3(b). Similar to the emission case, excitation (or absorption of light) of the nanotube is maximum around 0° corresponding to the electric field component of the laser excitation along the tube axis. Again the PL intensity did not reach zero, and the extinction ratio for excitation is in general smaller, ranging between 5 and 15. For the result of Fig. 3(b), the excitation polarization is flattened compared to the emission polarization, and a $[\cos^2\theta]^{0.7}$ functional form is a reasonable fit to the data. While the precise shape of the angular dependence differs somewhat, a similarly periodic polarization dependence of absorption was previously shown for the Raman spectroscopy of individual SWNTs, which were not suspended.[12]

The analytical power of mapping PL spectra as a function of the photon excitation energy (PL excitation or PLE) was introduced in Ref. 3. A similar result is presented in Fig. 4(a) for a large number of SWNTs bridging pillars in a uniform grid pattern.[9] The color plot in Fig. 4(a) of the PL intensity as a function of emission and excitation energies shows at least four peaks, each corresponding to a different species of SWNTs. Two peaks in particular have a greater intensity. This is likely due to a larger population, a higher absorption cross section, or greater luminescent efficiency of those species. Using the assignment scheme of Weisman and Bachilo,[13] these two peaks can be attributed to a (9,8) nanotube with emission/absorption at 0.904/1.550 eV, and to a (9,7) nanotube with emission/absorption at 0.964/1.588 eV. Their assignment scheme, derived semi-empirically from micelle encapsulated SWNT data, applies with little modification to nanotubes suspended in air.[14] That is, over a common range of excitation and emission energies, there is a one-to-one correspondence between peak positions for micelle encapsulated and pillar suspended nanotubes.

A similar color plot obtained for a single (9,8) SWNT is shown in Fig. 4(b). The spectrum is dominated by only one peak for the entire range of excitation and emission energies. The enhancement of luminescence intensity on resonance is typically 10 for the single nanotube measurement. It is larger than the ensemble average measurement where nonresonant emission from other nanotube species contributes to a nonzero background.

It is worth noting that the individual peak shape and the corresponding average over many nanotubes of the same species are qualitatively very similar. This is a striking result considering that ensemble average measurements in most

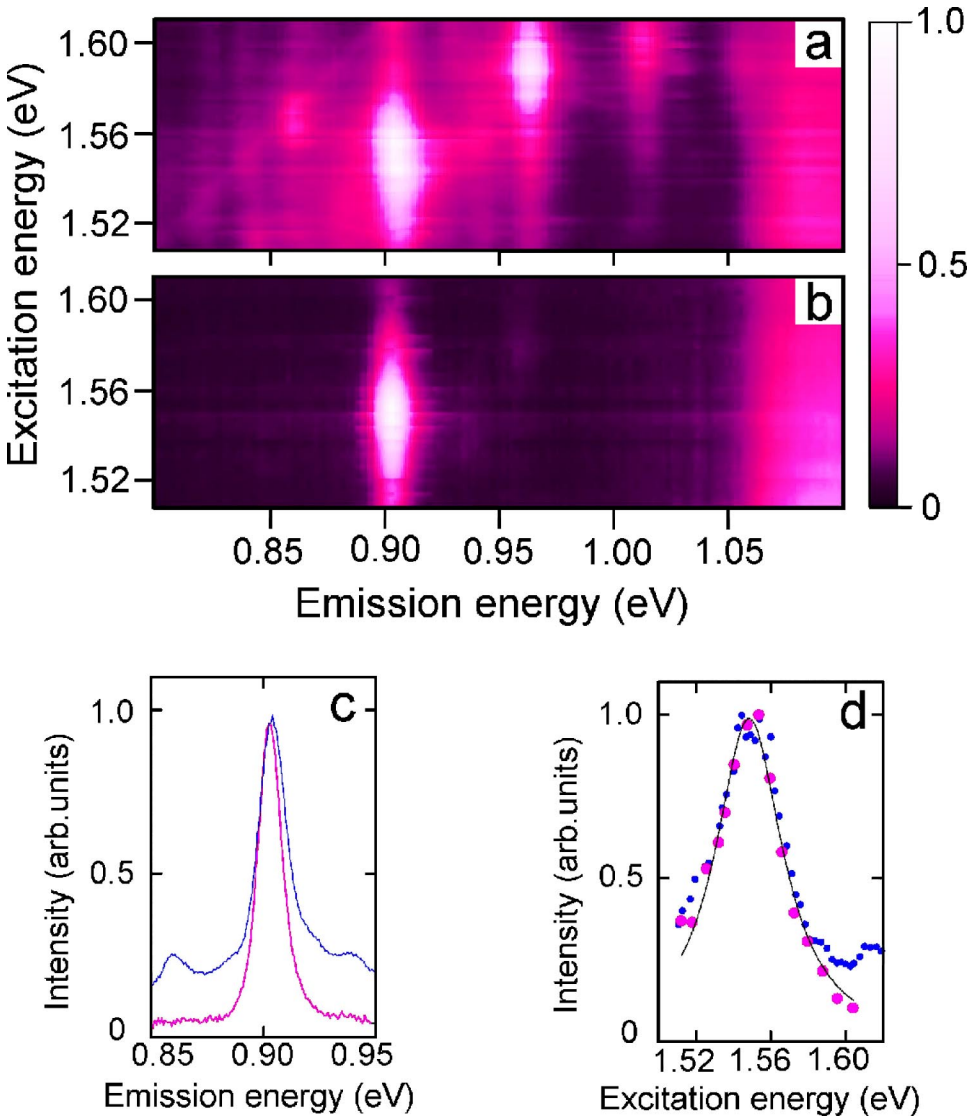

FIG. 4. Photoluminescence (PL) intensity as a function of emission and excitation energy. (a, b). Color plot of the PL intensity as a function of emission energy (x axis) and excitation energy (y axis). PL spectra are taken for different excitation wavelengths of a tunable Ti:sapphire laser (between 725 and 837 nm, 1 mW power). The brighter the color, the higher the intensity (see scale bar). (a) A spectrum obtained when probing an ensemble of many SWNTs, showing a finite set of peaks. Each peak arises from a specific SWNT species with a given diameter and chirality. The spot size is 100 μm in diameter, while pillars are in a grid with $\sim$0.5 μm spacing, with the result that $\sim 10^4$ SWNTs are probed. (b) A spectrum obtained when probing only one SWNT, using a $\sim$2 μm spot diameter on a pillar pair, showing a single peak that can also be seen in (a). The broad excitation independent peak with onset at 1.06 eV comes from the Si substrate. (c, d) PL intensity slices for a given excitation (c) and emission (d) energy. (c) PL intensity vs emission energy (horizontal slice at 1.548 eV) for the ensemble (blue) and single nanotube (red) measurement. The emission linewidth is 13 meV. (d) PL intensity vs excitation energy (vertical slice at 0.903 eV) for the ensemble (blue) and single nanotube (red) measurement. The excitation linewidth is 44 meV.

material systems lead to significant inhomogeneous broadening, and stands in stark contrast to a recent report of different PL peak energies for the same species of SWNT.[10] Figures 4(c) and 4(d), which are slices through the color plots, show the similarity graphically. In Fig. 4(c), the PL intensity as a function of emission energy (excitation at 1.554 eV) shows a 13 meV FWHM peak in both cases. In Fig. 4(d), the PL intensity as a function of excitation energy (detection at 0.903 eV) shows a 44 meV FWHM in both cases. The excitation linewidth is systematically two to three times broader than the emission linewidth (typically 35 meV versus 15 meV). A possible explanation for the difference between emission and excitation linewidths may be the much shorter lifetime of carriers in higher subbands.[15] However, it is also possible that the shape of the joint density of states in the neighborhood of the van Hove singularities may be wider for second subbands than it is for the lowest subbands. In the future, studies of the dynamics of optical absorption and emission, as well as temperature dependent PL, should be able to address this issue.

This work clearly demonstrates the potential of PL spectroscopy at the single nanotube level. An individual SWNT in air emits bright, sharp, asymmetrically peaked PL. In comparison to ensemble measurements, PL and PLE spectra

from an individual nanotube are greatly simplified, with a unique emission peak, and a corresponding set of absorption peaks. The one-dimensional character of nanotubes is clearly seen in luminescence data obtained at the single nanotube level: peak widths are narrower than the thermal energy, lineshapes are asymmetric, and both emission and absorption are strongly polarized. The SWNT is possibly the best experimentally accessible model of a one-dimensional system, and optical spectroscopy is a very effective tool to explore the physical consequences of the reduced dimensionality. Data from single SWNTs will complement ensemble data, and streamline the comparison of theory to experiment.

This work was carried out with assistance from the NEDO International Joint Research Grant Program. We are grateful to R. L. Williams (NRC) for helpful advice regarding PL measurements, and to D. Takagi (Meiji University) for performing a series of nanotube depositions.

*Author to whom correspondence should be addressed. Email address: jacques.lefebvre@nrc.ca

[1] *Carbon Nanotubes: Synthesis, Structures, and Applications*, edited by M. S. Dresselhaus, G. Dresselhaus, and Ph. Avouris (Springer, Berlin, 2001).

[2] M. J. O'Connel, S. M. Bachilo, C. B. Huffman, V. Moore, M. S. Strano, E. Haroz, K. Rialon, P. J. Boul, W. H. Noon, C. Kittrell, J. Ma, R. H. Hauge, R. B. Weisman, and R. E. Smalley, Science **297**, 593 (2002).

[3] S. M. Bachilo, M. S. Strano, C. Kittrell, R. H. Hauge, R. E. Smalley, and R. B. Weisman, Science **298**, 2361 (2002).

[4] J. Lefebvre, Y. Homma, and P. Finnie, Phys. Rev. Lett. **90**, 217401 (2003).

[5] C. Kane and G. Mele, Phys. Rev. Lett. **90**, 207401 (2003).

[6] A. Grüneis, R. Saito, Ge. G. Samsonidze, T. Kimura, M. A. Pimenta, A. Jorio, A. G. Souza Filho, G. Dresselhaus, and M. S. Dresselhaus, Phys. Rev. B **67**, 165402 (2003).

[7] I. Miloševic, T. Vukovic, S. Dmitrovic, M. Damnjanovic, Phys. Rev. B **67**, 165418 (2003).

[8] J. Kong, A. M. Cassell, and H. Dai, Chem. Phys. Lett. **292**, 567 (1998).

[9] Y. Homma, Y. Kobayashi, T. Ogino, and T. Yamashita, Appl. Phys. Lett. **81**, 2261 (2002).

[10] A. Hartschuh, H. N. Pedrosa, L. Novotny, and T. D. Krauss, Science **301**, 1354 (2003).

[11] J. A. Misewich, R. Martel, Ph. Avouris, J. C. Tang, S. Heinze, and J. Tersoff, Science **300**, 783 (2003).

[12] S. Duesberg, I. Loa, M. Burghard, K. Syassen, and S. Roth, Phys. Rev. Lett. **85**, 5436 (2000).

[13] R. B. Weisman and S. M. Bachilo, Nano Lett. **3**, 1235 (2003).

[14] J. Lefebvre, J. M. Fraser, Y. Homma, and P. Finnie, cond-mat/0308359, Appl. Phys. A (to be published).

[15] G. N. Ostojic, S. Zaric, J. Kono, M. S. Strano, V. C. Moore, R. H. Hauge, and R. E. Smalley, cond-mat/0307154 (unpublished).